Interorgan coordination of the murine adaptive response to fasting

THE JOURNAL OF BIOLOGICAL CHEMISTRY VOL. 286, NO. 18, pp. 16332–16343, May 6, 2011

Interorgan Coordination of the Murine Adaptive Response to Fasting*[S]

Received for publication, December 29, 2010, and in revised form, February 21, 2011 Published, JBC Papers in Press, March 10, 2011, DOI 10.1074/jbc.M110.216986

Theodorus B. M. Hakvoort[‡1], Perry D. Moerland[§¶1], Raoul Frijters[‖], Aleksandar Sokolović[‡], Wilhelmina T. Labruyère[‡], Jacqueline L. M. Vermeulen[‡], Emiel Ver Loren van Themaat[§], Timo M. Breit[¶], Floyd R. A. Wittink[**], Antoine H. C. van Kampen[§¶‡‡], Arthur J. Verhoeven[§§], Wouter H. Lamers[‡], and Milka Sokolović[§§2]**

*From the [‡]Tytgat Institute for Liver and Intestinal Research (formerly AMC Liver Center), Academic Medical Center, University of Amsterdam, Amsterdam 1105BK, the [§]Bioinformatics Laboratory, Department of Clinical Epidemiology, Biostatistics, and Bioinformatics, Academic Medical Center, University of Amsterdam, Amsterdam 1105AZ, the [¶]Netherlands Bioinformatics Centre, Nijmegen 1105AZ, the [‖]Computational Drug Discovery Group, Center for Molecular and Biomolecular Informatics, Radboud University Nijmegen Medical Centre, Nijmegen 6525GA, the **MicroArray Department and Integrative Bioinformatics Unit, Swammerdam Institute for Life Sciences, Faculty of Science, University of Amsterdam, Amsterdam 1090GE, [‡‡]Biosystems Data Analysis, Swammerdam Institute for Life Science, University of Amsterdam, Amsterdam, 1105AZ, and the [§§]Department of Medical Biochemistry, Academic Medical Center, University of Amsterdam, Amsterdam 1105AZ, The Netherlands*

Starvation elicits a complex adaptive response in an organism. No information on transcriptional regulation of metabolic adaptations is available. We, therefore, studied the gene expression profiles of brain, small intestine, kidney, liver, and skeletal muscle in mice that were subjected to 0–72 h of fasting. Functional-category enrichment, text mining, and network analyses were employed to scrutinize the overall adaptation, aiming to identify responsive pathways, processes, and networks, and their regulation. The observed transcriptomics response did not follow the accepted "carbohydrate-lipid-protein" succession of expenditure of energy substrates. Instead, these processes were activated simultaneously in different organs during the entire period. The most prominent changes occurred in lipid and steroid metabolism, especially in the liver and kidney. They were accompanied by suppression of the immune response and cell turnover, particularly in the small intestine, and by increased proteolysis in the muscle. The brain was extremely well protected from the sequels of starvation. 60% of the identified overconnected transcription factors were organ-specific, 6% were common for 4 organs, with nuclear receptors as protagonists, accounting for almost 40% of all transcriptional regulators during fasting. The common transcription factors were PPARα, HNF4α, GCRα, AR (androgen receptor), SREBP1 and -2, FOXOs, EGR1, c-JUN, c-MYC, SP1, YY1, and ETS1. Our data strongly suggest that the control of metabolism in four metabolically active organs is exerted by transcription factors that are activated by nutrient signals and serves, at least partly, to prevent irreversible brain damage.

Adapting to starvation requires an interorgan integration of the activity of metabolic pathways to protect the body from an irreversible loss of resources (1, 2), but how the organism integrates these reactions remains largely unknown. Numerous studies on humans, who fasted for 3–6 weeks, have shown that glycogen stores are depleted within a day (3). The decline in circulating glucose and insulin during the next few days (4) induces a transient increase in plasma (essential) amino acids and a concomitant decline in plasma alanine levels due to an increased hepatic extraction for gluconeogenesis (5, 6). Muscle catabolism is a major source of amino acids in this phase. When fasting is continued, muscle protein catabolism declines, and hepatic uptake of amino acids decreases, which is reflected in a decline of endogenous glucose production (6) and urinary nitrogen excretion (4, 7). Lipid catabolism and the (hepatic) production of ketone bodies also increases rapidly and is quantitatively similar after 3 days and 5–6 weeks of starvation (8), but plasma levels increase only gradually to plateau after 4 weeks (4, 9). The associated increase in urinary ketone body (organic-acid) excretion requires a compensatory increase in ammonia production and urinary excretion (4, 7, 10), which is met by an increased renal amino acid uptake and gluconeogenesis (5, 6). As a result, the kidney and the liver produce similar amounts of glucose (4, 6) and ammonia/urea (7) after 2–3 weeks of fasting. From the third week onward, the circulating level of β-hydroxybutyrate has become sufficiently high to replace glucose as the fuel in *e.g.* the central nervous system (11), but amino acids continue to be catabolized at a low rate (12) because some tissues (erythrocytes) need glucose as fuel, whereas the kidney needs to produce ammonia. This large body of metabolomic data describes an essentially biphasic response with an early phase in which proteins and fats are equally used as energy sources and a late phase in which proteins are maximally conserved.

* This study was supported by Dutch Ministry of Economic Affairs through the Innovative Oriented Research Program on Genomics (IOP Genomics IGE01016) and by a grant T2-110 from Top Institute Pharma.

[S] The on-line version of this article (available at http://www.jbc.org) contains supplemental Tables 1–4, Files 1–10, and Figs. 1 and 2.

The data discussed in this publication have been deposited in NCBI Gene Expression Omnibus (25) in a MIAME compliant format and are accessible through GEO Series accession number GSE24504.

[1] Both authors contributed equally to this work.

[2] To whom correspondence should be addressed: Dept. of Medical Biochemistry, Academic Medical Center, University of Amsterdam, P. O. Box 22700, 1100 DE, Amsterdam, The Netherlands. Tel.: 31205665136; Fax: 31206915519; E-mail: m.sokolovic@amc.uva.nl.

Relatively few studies on prolonged fasting in mice are available, but in aggregate, the metabolomic data reveal both similarities and differences with humans. We quantified a number of metabolites in our previous fasting-related studies (13–16). Plasma ammonia levels increased ~5-fold with the duration of fasting in mice, whereas plasma β-hydroxybutyrate increased >10-fold to a plateau of 1–2 mM after 24 h of fasting (14, 16, 17). Plasma glucose and lactate concentrations declined transiently at 36 and 48 h of fasting to return to prefasting levels at 72 h of fasting (14). Supporting the validity of the increase in plasma glucose levels was the initial depletion of glycogen in the liver followed by a progressive reaccumulation in the pericentral, that is, non-gluconeogenic part of the liver (14). Similarly, many amino acids (alanine, serine, histidine, glycine, arginine, citrulline, and phenylalanine) transiently declined at 24 and 48 h of fasting to return to prefasting levels at 72 h, whereas branched-chain amino acids, threonine, asparagine, and taurine increased in concentration with the duration of fasting. These data concur with human data to the extent that increasing ammonia levels probably reflect increasing renal production and excretion to compensate for the increased organic acid (β-hydroxybutyrate) excretion. However, the transient decline in glucose, lactate, and most amino acids clearly differs from the findings in humans during prolonged fasting and still need further research to be clarified. A subsequent study (15), which focused on lipid metabolism, showed that the plasma concentration of cholesterol increased and that of triglycerides decreased to new levels within 24 h, whereas fecal cholesterol output declined progressively with the duration of fasting. Hepatic triglyceride concentration increased after 24 h, and hepatic and intestinal cholesterol and phospholipid concentrations increased after 48 h of fasting. Furthermore, we observed an increase in biliary cholesterol, bile salt, and phospholipid excretion, which we believe serves to nourish enterocytes from the luminal side.

During the initial phase of fasting the rate of weight loss is high but then declines to a minimum until the final, moribund phase with more rapid weight loss sets in (18, 19). Based on whole-body energy expenditure, these three phases of weight loss were interpreted as reflecting successively the postabsorptive utilization of glycogen reserves, oxidation of fat (with a protein-sparing effect), and eventually the self-destructive consumption of cell proteins (18, 20). However, transcriptomics data from fasting muscle, small intestine, and liver (13, 14, 21) suggest that increased protein degradation is an early response in muscle that is accompanied by a temporary suppression of glutamine consumption in the intestine and an up-regulation of gluconeogenic enzymes in the liver. The late response of the intestine is primarily directed to cell survival, whereas this phase is (unexpectedly) characterized by a near-normalization of carbohydrate metabolism in liver. Although data on long term starvation in muscle, kidney, and brain are not available, these transcriptomic data in rodents appear to concur with the human metabolomic data that protein conservation during fasting follows an initial phase during which protein catabolism is liberally used to produce glucose and to contradict the sequential model in which protein catabolism is a terminal step in long term fasting.

This study aims to test the hypothesis that the adaptive response of a mouse to prolonged fasting involves an integrated interorgan program of progressive metabolic adaptations that subserves the maintenance of vital organ functions. The question was addressed with a systems biology approach using transcriptomics and advanced bioinformatics to analyze the adaptive expression signatures of the small intestine, liver, kidney, muscle, and brain. By analyzing the transcriptomes of five organs at five different time points, we could produce a comprehensive view of the pathways, processes, and networks that mediate this adaptive response. Our findings show that the adaptive responses do not favor a succession of substrates used for energy expenditure, but that pathways catabolizing carbohydrates, fats, and proteins were activated simultaneously in different organs. The most prominent changes occurred in lipid and steroid metabolism accompanied by suppression of the immune response and cell turnover. Brain appeared to be well protected against fasting. The result identified a set of transcription factors that may mediate the spatiotemporal regulation of general metabolism, cell turnover, and immune response in response to fasting.

EXPERIMENTAL PROCEDURES

Animals and Organs— 6-Week-old male FVB mice (Charles River, Maastricht, The Netherlands) were fasted for 0, 12, 24, 48, or 72 h before sacrifice ($n = 8$ per group; the 12-h group was fasted overnight). 24 h before and during fasting, the animals were kept in metabolic cages to prevent the consumption of bedding and feces and were kept warm with an infrared lamp. Body weight was determined daily. The daily rate of body- and organ-mass loss was calculated in comparison to the previous time point as described (22). Before organ harvesting (between 9:00 and 10:00 a.m.), the animals were anesthetized with 1.25 mg of ketamine and 2 μg of dexmedetomidine per 10 g of body weight in 0, 12, and 24 h fasted and with a 20% reduced amount in 48 and 72 h fasted mice. After blood collection (lithium heparin) from the inferior caval vein, mice were killed by decapitation. The organs (brain, kidney, liver, small intestine, and calf muscle) were quickly isolated, weighed, snap-frozen in liquid nitrogen, and stored at −80 °C. The entire procedure was carried out by five operators to expedite organ isolation and prevent RNA degradation. The animal studies were reviewed and approved by the AMC committee for animal care and use.

RNA Isolation—Total RNA was extracted from the frozen organs of eight animals per experimental group with TRIzol reagent (Invitrogen) followed by a repeated phenol-chloroform extraction, LiCl precipitation, and additional purification using the RNeasy Mini kit (Qiagen Benelux, Venlo, The Netherlands). The RNA quality was assessed using the RNA 6000 Nano LabChip® kit in an Agilent 2100 bioanalyzer (Agilent Technologies, Palo Alto, CA). All samples had intact bands corresponding to 18 S and 28 S ribosomal RNA subunits, displayed no chromosomal peaks or RNA degradation products, and had an RNA integrity number >8. Five of eight animals per group were chosen based on the best RNA quality across all five tissues, so

that the RNAs used in this study all originated from the same five mice per time point.

Microarrays—125 microarrays (5 time points, 5 mice per time point, 5 tissues) were performed. We used a common-reference design shown to be robust to low quality arrays, amenable to clustering, and allowing for comparison of more than two conditions at once without dye effects (23). The single common-reference sample, a pool of equal amounts of RNA from all the samples investigated, was used in all arrays to allow for quantitative comparisons across time points and tissues.

The microarray labeling and hybridization were performed at the Microarray Department, University of Amsterdam. Labeling and hybridization days were organized so that all comparisons could be analyzed with minimal confounding. One experimental block containing all 25 samples per tissue was too large to handle in a day. The blocks were, therefore, randomized so that the same time points were not labeled/hybridized on the same day. The Cy3-labeled test samples were hybridized against the common-reference sample (Cy5-labeled) using Microarray Department two-dye home-spotted arrays, printed with the 22K 65-mer Sigma/Compugen Mouse OligoLibrary™ with the oligo library reannotated as described (24).

Data Preprocessing, Clustering, and Statistical Analysis—All analyses were carried out with packages from Bioconductor (26) in the statistical software package R (Version 2.6.1). Estimated foreground and background signals were extracted from the ArrayVision files. Two arrays did not pass our quality control performed on the raw data due to spatial artifacts.

Background correction was performed using the "normexp" method (27) to adjust the foreground signal without introducing negative values. The resulting log ratios were normalized per array by print-tip loess. Because some of the control probes, notably *Gapdh*, showed substantial between-tissue variation, they were down-weighted to zero in the normalization step. The statistical analysis of the data was performed within each tissue separately by comparing 0 h *versus* all other time points. Each probe except the controls was tested for any change in expression over the 5 time points with a moderated F-test. Differential expression for the pairwise comparisons between 0 h and any of the other time points was assessed using a moderated *t* test. Moderated tests are similar to the standard tests for each probe, except that the standard deviations are moderated across genes to ensure a more stable inference for each gene. This prevents a gene from being judged as differentially expressed with a very small -fold change merely because of an accidentally small residual standard deviation (28). The resulting *p* values were corrected for multiple testing using the Benjamini-Hochberg False Discovery Rate adjustment. Genes were considered to be differentially expressed if the corrected *p* values were <0.05 (while controlling the expected false discovery rate to no more than 5%). Unsupervised hierarchical clustering was performed both on the raw data, as a quality control, and on normalized data, with complete linkage and Pearson's correlation distance.

Functional Category Enrichment Analyses—Identification of overrepresented functional categories (pathways and processes) was performed per tissue using the complete set of differentially expressed genes per time point (corrected $p < 0.05$, moderated *t* test) in the MetaCore™ suit (Version 6.1; GeneGo, Inc., St. Joseph, MI (29, 30)). The functional analysis of the data were based on MetaCore's proprietary manually curated data base of protein-protein and protein-DNA interactions, transcription factors, signaling, and metabolic pathways. Overrepresented functional categories were identified as described (31).

Network and Interactome Analyses—To study the regulation of the responsive genes, we performed network analysis in MetaCore™ using two different algorithms, which both deliver lists of subnetworks (one per transcription factor) but begin from a different start point. The "transcriptional regulation" algorithm starts with a small sub-network of differentially expressed genes from the initial list and adds the "responsible" transcription factors. The "transcription-factor target modeling" algorithm starts with list of transcription factors deduced from the initial dataset and calculates the shortest paths to their targets (31). The networks were generated for all five tissues using unions of differentially expressed genes (corrected $p < 0.05$, moderated *t* test).

To identify the major transcriptional regulators in the dataset, we used the statistical Interactome tool in MetaCore™. It calculates relative connectivity (number of interactions) of individual genes within the dataset compared with the entire data base based on the comprehensive collection of their known interactions (31). A gene was considered overconnected if it had more direct interactions with the genes of interest than it would be expected by chance (32). The related statistics are described in detail elsewhere (31). Shortly, to assess significantly over- or under-connected proteins in the list, Interactome analysis evaluates relative connectivity of proteins based on the assumption that the most critical protein in a given dataset has more connections within the dataset than expected at random. The interactions between proteins within a dataset (local interactome) are compared with general connectivity within the interactions data base (global interactome). Statistical significance is assigned by using the cumulative hypergeometric distribution as

$$p(k) = \sum_{i=k}^{D} P(i,D,n,N), \qquad \text{(Eq. 1)}$$

where

$$P(k,D,n,N) = \frac{\binom{D}{k}\binom{N-D}{n-k}}{\binom{N}{n}} \qquad \text{(Eq. 2)}$$

N is the number of proteins (protein-based network objects) in global interactome extracted from MetaCore, n is the number of proteins derived from the sets of genes of interest, D is the "degree" or number of interactions of a given protein in the global interactome data base, and k is the degree of a given protein within the set of interest. The p value calculated above gives the probability of observing k or more interactions of a given protein (with degree D in the global network) by random chance within the set of interest (of size n). The probability of

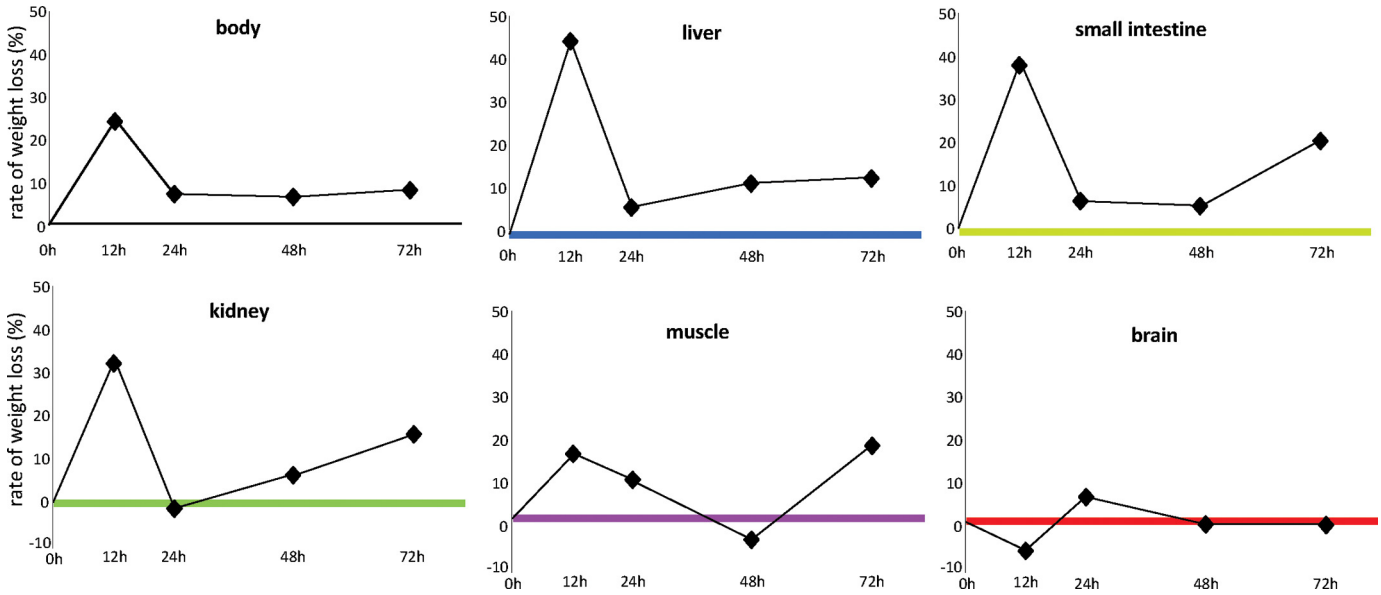

FIGURE 1. **Rate of weight loss of body and organs during fasting.** The rate of weight loss is calculated in comparison to the previous fasting time point and expressed as percent change in weight per day. Whole-body weight loss and that of the three visceral organs was significant ($p < 10-3$) at all the time points compared with that in non-fasted mice. Muscle weight loss became significant only after 72 h ($p < 0.004$), whereas no significant weight loss was seen in the brain.

observing under-connected proteins can be calculated by $1 - p(k)$. The resulting network of common and organ-specific regulators of fasting was created and visualized in Cytoscape (33) and graphically enhanced in Adobe Illustrator CS2.

Text Mining—The CoPub text mining tool, which extracts relationships between genes and keywords (*e.g.* pathways, diseases, drugs, and Gene Ontology (GO) terms) from literature (34, 35) was used to substantiate the transcriptomics findings. CoPub calculates an *R*-scaled score between two co-occurring concepts (*i.e.* genes and keywords) in Medline abstracts to assign a degree of relatedness between the two concepts (ranging from 0–100, representing non- to strong-association). It takes into account the number of co-publications between two concepts and the number of times each concept is separately mentioned in literature (34–36). For each tissue, a keyword enrichment analysis was performed to detect keywords significantly associated with the set of differentially expressed genes (raw $p < 0.01$, moderated F-test). A keyword was regarded as associated with a gene if it was co-mentioned in at least three abstracts and had an R-scaled score of at least 35. Furthermore, at least 10 regulated genes needed to be associated with a keyword to include it in the keyword-enrichment analysis. Keywords were regarded as enriched if $p < 0.01$ in the Fisher's exact test. The CoPub web server is publicly available online.

A proof of principle validation of text mining analysis by using publicly available datasets described and deposited at GeneNetwork is described in supplemental File 1. The file also contains a proof of principle validation of pathway analysis and descriptions of all the supplemental files and figures.

RESULTS

Body and Organ Weight Loss upon Fasting—Provided they are kept warm, mice withstand 72 h of fasting without problems and are still actively cruising their cage and hanging upside-down from the top. Similar to our previous studies (13, 14), the rate of body weight loss upon fasting was highest during the first 12 h. During this period the mice lost 12% of their initial weight (Fig. 1), *i.e.* approximately a quarter when expressed on a per-day basis (our common denominator for the 12- and 24-h-fasted animals). From 12 to 24 h, the weight loss was only ~8% per day and remained that low between 24 and 72 h so that the animals had lost ~30% of their initial weight after 3 days of fasting. Confirming our previous findings, a preterminal increase in the rate of body weight loss (as seen in *e.g.* rats (20)) was not observed. The liver, small intestine, and kidney followed a similar trend, albeit that weight loss gradually became more pronounced as fasting lasted longer. In total, these visceral organs lost 40–50% of their weight in 72 h. The decrease in body weight and that of the three visceral organs was significant ($p < 0.001$) at all the time points compared with that in non-fasted mice. The weight loss of calf muscle was a moderate 10–15% per day on the first 2 days of fasting and became significant on the third day only ($p < 0.004$). In total, muscle weight loss amounted to ~30%. Of note, the brain was protected from weight loss even during prolonged fasting.

Global Changes in Organ Transcriptomes during 3 Days of Fasting—The unsupervised hierarchical clustering of the raw microarray data revealed that all but one microarray clustered according to the organ from which the RNA was extracted (not shown), demonstrating that biological variation exceeded technical variation and that the overall quality of the microarray experiment was good. The non-fitting array (from liver, clustering with brain) was excluded from further analysis. Unsupervised hierarchical clustering of the normalized microarray data using 5237 genes differentially expressed in any of the tissues (Fig. 2) confirmed clustering of arrays according to the organs from which they originated. It further revealed 10 distinct clusters of genes, pointing both to the existence of concurrent multiorgan responses (*e.g.* clusters 1, 2, 3, and 9) and to tissue-

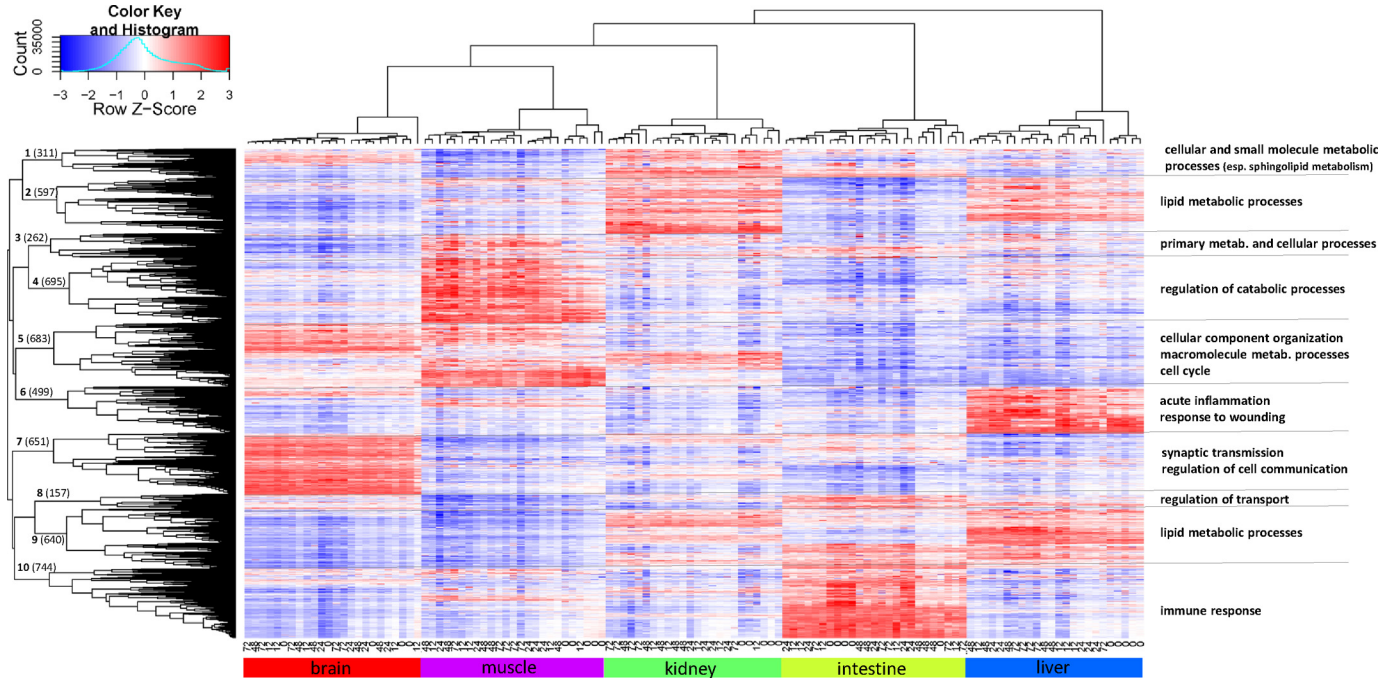

FIGURE 2. **Unsupervised hierarchical clustering of normalized microarray data.** Clustering of 122 microarrays that passed quality control was performed using complete linkage and Pearson correlation distance on the 5237 genes that were differentially expressed in any of the tissues. The Z-score is calculated on the rows by subtracting the mean expression value of the row from each of the values and then dividing the resulting values by the standard deviation of the row. Color in the heat maps, therefore, indicates the relative gene expression level, with *red* being higher and *blue* lower than the mean expression value. Number of genes belonging to the 10 clusters is given on the corresponding branches of the dendrogram. Major Gene Ontology processes overrepresented in those clusters are summarized on the *right*.

specific responses to fasting (*e.g.* clusters 4, 6, 7, and 10). Gene Ontology categories (37) statistically over-represented in these clusters are summarized in Fig. 2 and shown in detail in supplemental File 2.

To determine the dynamics of the transcriptional response in different tissues, each of the time points (12, 24, 48, and 72 h) was compared with the fed condition (0 h) for each of the organs studied. During the entire fasting period, (only) 45 genes in the brain, 656 in the small intestine, 1252 in the kidney, 2068 in the liver, and 3057 in the muscle were differentially expressed in a significant manner. Complete lists of differentially expressed genes are shown in supplemental File 3. The total number of differentially expressed genes (corrected $p < 0.05$) increased with the duration of fasting in each organ (Fig. 3*A*, *left panel*). The changes detected at each time point in comparison with the preceding time point (Fig. 3*A*, *right panel*) revealed the magnitude of the response during the first 12 h and the additive effect of the later periods. To introduce the direction of the changes in gene expression, we created heat maps of differentially expressed genes for each of the organs (Fig. 3*B*), with the significance threshold set to a corrected $p < 0.05$. The figure clearly demonstrates that the response in all organs increased with the duration of fasting. Notably, the direction of regulation of majority of the genes within an organ remained unchanged (*horizontal red* or *green lines*).

Pathways and Processes Affected by Fasting in Functional-categories Enrichment Analyses—To counteract an undue influence of post-transcriptional regulation on our conclusions, we have focused on pathways and networks rather than on individual genes as the dependable read-out of microarray analyses. We performed functional-categories enrichment analyses in the MetaCore™ suit to produce a comprehensive overview of the canonical pathways and processes altered by fasting. Table 1 shows the 10 most prominently regulated pathways in four of the metabolically highly active organs, with all the differentially expressed genes during fasting taken into consideration (the complete lists of regulated pathways are presented in supplemental File 4). Cholesterol biosynthesis was the only significantly (down) regulated canonical pathway in the brain ($p < 10^{-4}$), whereas significant changes in 35, 54, 69, and 141 GeneGo canonical pathways were found in intestine, kidney, liver, and muscle, respectively. Clearly, the most prominent changes in brain, liver, kidney, and intestine occurred in steroid metabolism, in particular that of cholesterol, bile acids, and steroid hormones. In kidney and liver, changes in expression of lipid-metabolizing genes were very prominent, whereas in intestine and muscle and to a lesser extent kidney, changes in expression of immune-response genes were notable. Cell-cycle regulating genes were highly affected in the intestine, and cell-structure modulating genes were prominently changed in muscle and intestine. Changes in the expression of amino acid metabolizing genes were mostly present in kidney, liver, and muscle. When these changed canonical pathways were grouped, five metabolic processes, as defined by MetaCore™ (*i.e.* amino acid, carbohydrate, lipid, steroid, and co-factor metabolism), emerged as the main affected features. The outcome of enrichment analysis for Gene Ontology categories was in excellent concordance with these data (not shown).

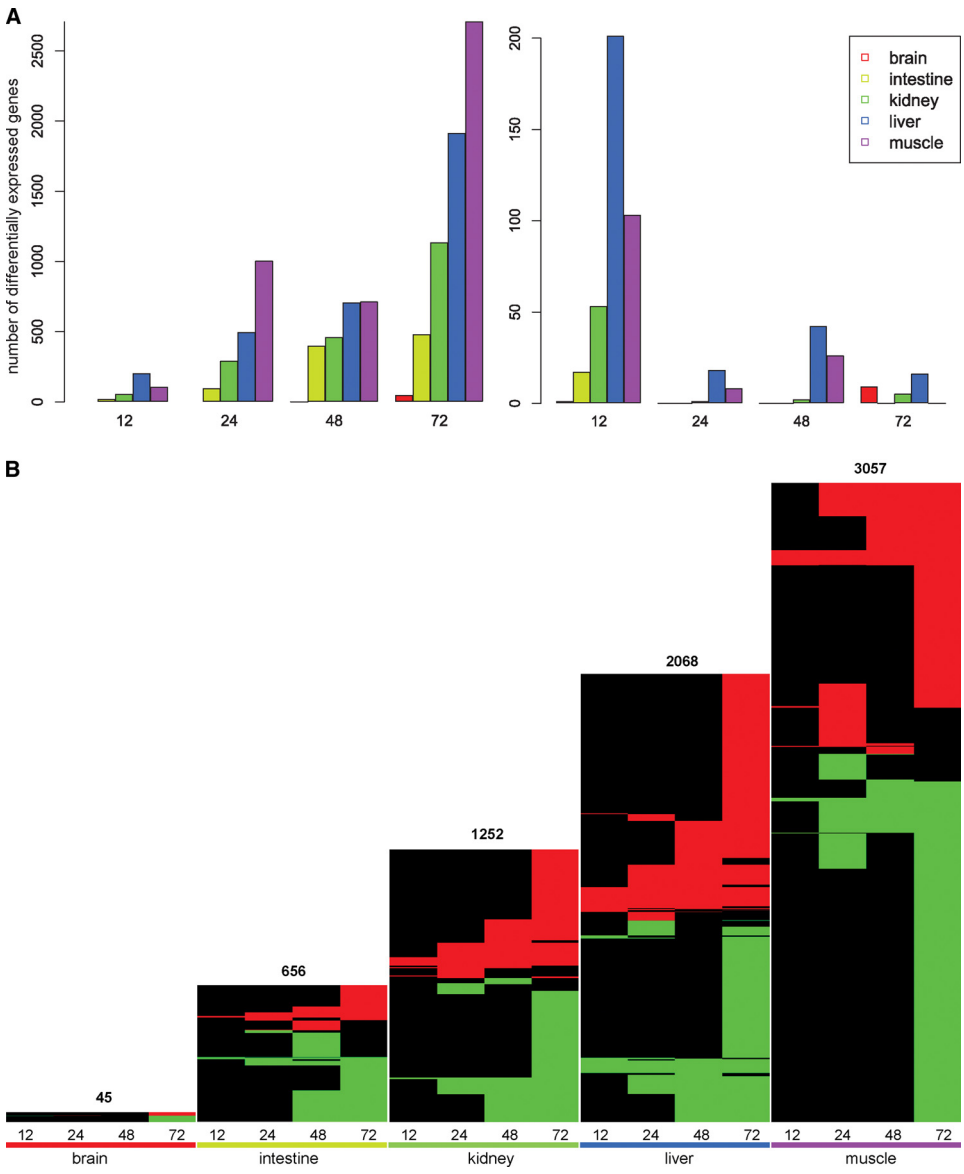

FIGURE 3. **Number of differentially expressed genes per time point of fasting.** *Panel A*, shown is number of genes that are differentially expressed (corrected $p < 0.05$) in comparison with 0h fasting (*left panel*) and in comparison with the previous time point of fasting (12 *versus* 0, 24 *versus* 12 etc.; *right panel*). Fasting generated a progressive adaptive response, but the most pronounced changes occurred during the first 12 h. *Panel B*, shown are heat maps containing all differentially expressed genes in five organs at four fasting conditions. In each heat map a row represents a single gene, with *red* depicting significant up-regulation, and *green* depicting significant down-regulation. *Black* indicates no differential expression at that time point. Genes with similar behavior across time (within an organ) are clustered together using complete linkage and Euclidean distance. The height of heat maps is scaled to (indirectly) reflect the number of genes.

To demonstrate the spatiotemporal coordination of different processes, we created a heat map with processes on one axis and organs/time points on another axis depicting the significance of the changes (Fig. 4*A*). The heat map demonstrates clear dominance of lipid and steroid metabolism, in particular in the liver and kidney. Vitamin and cofactor metabolism comprises a number of pathways, *e.g.* vitamin E and niacin-HDL metabolism, which only add weight to the importance of lipid metabolism. The heat map further reveals that the multiple processes were activated simultaneously in an organ and remained active during the entire fasting period, stressing the interrelatedness of the response across time and tissues. The current study detects the biphasic response of carbohydrate metabolism in the intestine and its attenuation in prolonged fasting in the liver (as seen in our previous studies (13, 14)), but no obvious overall temporal trend in pathway regulation emerged.

To provide a substantiation of the outcome of the functional category enrichment analysis, we tested one of the hypotheses generated by this approach; that is, ketone body synthesis in the fasted small intestine, a feature not previously linked to this organ in adults. This biosynthetic process is usually associated with the liver and kidney and was only observed in the small intestine of newborn mice before weaning (38). We measured the β-hydroxybutyrate concentration in intestinal perfusates from up to 48 h fasted mice from our previous study (15). Although it was not present in detectable levels in the intestinal lumen of fed animals, supplemental Fig. 1 demonstrates

TABLE 1

Ten most prominently regulated canonical pathways in response to fasting

MIF, macrophage migration inhibitory factor; GPCR, G protein-coupled receptor; APC, adenomatosis polyposis coli; SCF, stem cell factor; WNT, Wnt (wingless-related MMTV integration site) protein superfamily.

Pathway	*P* value	Objects	
		Changed	Out of
Intestine			
Immune response; antigen presentation by MHC class I	8.06E-06	10	26
Cytoskeleton remodeling; regulation of actin cytoskeleton by Rho GTPases	1.55E-04	8	23
Immune response; CCR3 signaling in eosinophils	1.06E-03	12	59
Immune response; MIF, the neuroendocrine-macrophage connector	1.48E-03	8	31
Blood coagulation; GPCRs in platelet aggregation	1.69E-03	11	54
Cell cycle; role of APC in cell cycle regulation	1.85E-03	8	32
Cholesterol biosynthesis	3.36E-03	6	21
Cell cycle; the metaphase checkpoint	4.10E-03	8	36
Oxidative stress; role of ASK1 under oxidative stress	4.34E-03	6	22
Cell cycle; role of SCF complex in cell cycle regulation	4.40E-03	7	29
Kidney			
Peroxisomal branched chain fatty acid oxidation	1.63E-06	12	22
Vitamin E (α-tocopherol) metabolism	5.04E-06	10	17
Peroxisomal straight-chain fatty acid β-oxidation	2.99E-05	7	10
Triacylglycerol metabolism	3.03E-04	11	29
Translation; regulation of translation initiation	3.46E-04	10	25
Cholesterol biosynthesis	3.73E-04	9	21
Mitochondrial long chain fatty acid β-oxidation	5.95E-04	8	18
Bile acid biosynthesis	1.36E-03	10	29
Immune response; MIF, the neuroendocrine-macrophage connector	2.40E-03	10	31
Polyamine metabolism	2.81E-03	8	22
Liver			
Cholesterol biosynthesis	5.53E-06	13	21
Peroxisomal branched chain fatty acid oxidation	1.14E-05	13	22
Lipoprotein metabolism I; chylomicron, VLDL and LDL	2.98E-05	7	8
Lipoprotein metabolism II; HDL metabolism	2.98E-05	7	8
Translation; regulation of translation initiation	7.16E-05	13	25
Androstenedione and testosterone biosynthesis and metabolism	7.24E-05	11	19
Triacylglycerol metabolism	1.08E-04	14	29
Estrone metabolism	1.11E-04	9	14
Vitamin E (α-tocopherol) metabolism	1.31E-04	10	17
Aspartate and asparagine metabolism	2.42E-04	11	21
Muscle			
Cytoskeleton remodeling	1.01E-06	42	96
Cytoskeleton remodeling; TGF, WNT, and cytoskeletal remodeling	1.11E-05	43	107
Immune response; antigen presentation by MHC class I	1.35E-05	16	26
Immune response; oncostatin M signaling via MAPK	1.72E-05	20	37
Neurodisease; Parkin disorder under Parkinson disease	1.80E-05	17	29
Proteolysis; role of Parkin in the ubiquitin-proteasomal pathway	1.09E-04	14	24
G-protein signaling; Ras family GTPases in kinase cascades	1.09E-04	14	24
Cell adhesion; chemokines and adhesion	1.44E-04	36	93
Transcription; Transcription regulation of amino acid metabolism	1.99E-04	14	25
Cytoskeleton remodeling; role of PKA in cytoskeleton reorganization	2.49E-04	16	31

increasing concentrations of this ketone body in the intestinal lumen of mice with longer durations of fasting. This finding, which is in good accordance with the increased excretion of biliary lipids in the same study, corroborates the hypothesis that the fasting small intestine acquires the capability to synthesize ketone bodies (most likely using biliary phospholipids as substrate).

Processes Differentially Regulated by Fasting as Revealed by Text Mining Analyses—To substantiate the above findings from a different perspective, CoPub keyword-enrichment analysis was performed using sets of differentially expressed genes per tissue. In total, 7, 50, 94, 76, and 82 keywords were significantly enriched in brain, intestine, kidney, liver, and muscle, respectively (supplemental File 5). For an easier overview, we grouped them into 28 higher order categories with amino acid, fat, carbohydrate, energy, steroid and drug metabolism, immune response, cell turnover, and protein metabolism containing most of the enriched keywords. Results of the CoPub analysis of these new (higher order) keywords are shown in supplemental File 6. Fig. 4*B* presents a heat map depicting the significance of keyword enrichment for these groupings for each organ. Similarly to the fasting adaptations detected by the analysis shown in Fig. 4*A*, fat and steroid metabolism noticeably dominated the response. Carbohydrate metabolism, however, came out more prominently regulated than in the MetaCore™ analysis. Amino acid, energy, protein, and oxidative-stress metabolism responded significantly to fasting in most organs. Apart from the metabolic adaptations, cell turnover was significantly regulated in the small intestine and muscle. Keywords linked to immune defense were enriched in the small intestine. In the brain, as by now expected, very few higher order categories were found significantly represented (only cholesterol and drug metabolism and neuronal signaling). Interestingly, based on the gene expression profiles of these organs, the concept "fasting" *per se* was enriched in kidney and liver.

We further performed a complementary, directed text mining analysis to identify fasting-related genes in the set of all differentially expressed genes. They were filtered from this set based on the literature co-occurrence with the keywords "fasting," "caloric restriction," "cachexia," and "food deprivation"

(for a complete list see supplemental File 7). Phosphoenolpyruvate carboxykinase 1 (*Pck1*)[3] emerged as one of the most frequently cited fasting-induced genes in liver and kidney. It was also up-regulated in the small intestine together with glucose-6-phosphatase (*G6pc*), indicating yet again (13, 39) the gluconeogenic potential of this organ after prolonged fasting. In addition, the fasting-associated FoxO transcription factors, in particular *FoxO1* and *FoxO3a*, were up-regulated in kidney, liver, and muscle. *Pgc-1α*, a *FoxO3a* co-activator (40), was also up-regulated in the long-fasted kidney and muscle. In the small intestine, the *FoxO* transcription factors were not regulated *per se*, but some of their targets (*Pck1* (41) and *G6pc* (42, 43)) were. Furthermore, adiponectin receptors 1 and 2 (*Adipor1* and *-2*), which regulate glucose uptake and lipid catabolism (44, 45) and were thus far mainly linked to obesity, also came prominent out of this analysis. We now show them regulated in fasting in all the studied tissues except kidney.

To demonstrate the validity of the text mining approach, we analyzed the correlation of the mRNA abundance of *FoxO1* in the livers of BxD genetic reference mouse population (obtained by 20-generation inbreeding in the F2 mice from an intercross between C57BL/6J and DBA/2J strains (Ref. 46, GeneNetwork and supplemental File 1) and its relationship with fasting glucose levels (47). A remarkable negative correlation ($r = -0.90$) was found between FoxO1 expression and glucose concentration (supplemental Fig. 2). Interestingly, the second (among the top-scoring 500) gene-phenotype correlation for *FoxO1* was that with the lean body mass ($r = -0.85$ (47)). These relationships underline our hypothesis that FOXO1 may play a key role in response to nutrient deprivation and, by implication, to weight loss upon fasting.

Transcriptional Regulation of the Fasting Response by Network and Interactome Analyses—To study the regulation and biological connectivity of fasting-responsive genes in five different tissues, we performed network analyses for transcriptional regulation and transcription factor-target modeling in the MetaCore™ suite. A list of networks (separate for each transcription factor emerging from our fasting data) was built for brain, intestine, kidney, liver, and muscle using two different approaches (supplemental Files 8 and 9). The two different algorithms (detailed under "Experimental Procedures") gave similar outcomes. By manually delineating the most prominent hubs in a number of top scoring networks from both lists, we obtained a list of transcription factors that was in surprisingly close agreement with the overconnected genes obtained subsequently from the Interactome analysis.

To quantify the overconnectivity of the hubs as major features of these networks and, thereby, the key regulators of fasting response, we performed Interactome analysis using MetaCore. By evaluating changes in gene expression in the context of a comprehensive data base of molecular interactions, this analysis identifies regulatory components of the biological networks that represent critical hubs driving the observed gene expression changes that do not necessarily have to be changed in expression themselves. The highly interconnected transcription factors in each of the tissues in fasting are shown in supplemental File 10. Almost 60% of the over-connected transcription factors were unique for an organ, of which almost 90% were specific for muscle. 40% of the transcription factors were common for at least 2, 20% for at least 3, and 6% for at least 4 organs. The network that links the common and organ-specific regulators with the corresponding organs is shown in Fig. 5. It revealed SREBP1 as the only transcriptional regulator highly interconnected in all five tissues in fasting. Furthermore, a set of TFs (SREBP2, the nuclear-hormone receptors AR (androgen receptor), GCRα, PPARα, and HNF4α, and C-JUN, SP1, C-MYC, YY1, ETS1, and EGR1) appears to orchestrate the fasting response in four metabolically highly active organs. In keeping with the fact that major regulators of lipid metabolism, such as HNF4α and SREBP1, were the major hubs of several top scoring networks in the liver, a whole set of network members responsive to lipid levels, like *Car*, *Pxr*, *Pparα*, and *Lrh*, was up-regulated in this organ. Similarly, a number of nuclear receptors were up-regulated in muscle (*e.g. Rorα*, *Rorγ*, *Rarβ*, and *Cebpδ*). Interestingly, in addition to FOXO1 and FOXO3A, pointed out by our CoPub text mining, the Interactome analysis revealed four other members of forkhead gene family as major regulators of fasting response (FOXM1 in the intestine, FOXK1 in muscle, and FOXD3 and FOXQ1 in the liver).

DISCUSSION

The adaptive response to fasting in major organs has been studied extensively (>65,000 hits in PubMed) but usually per function and per organ. The absence of comprehensive studies of the transcriptional adaptations to fasting is the more surprising in view of the extensive studies on humans that were cited in the Introduction and recently reviewed (3). Our study aimed to deduce factors that regulate the metabolic integration between the organs from gene expression profiles. They revealed that carbohydrate, fat, and protein catabolism were activated concurrently, although the features and intensities of their response were specific for each of the studied organs. The most prominent changes in the four metabolically highly active organs (especially liver and kidney) occurred in lipid and steroid metabolism. They were accompanied by suppression of the immune response and cell turnover in intestine and muscle and a generally enhanced defense against oxidative damage, probably to cope with the highly increased fat oxidation. Brain, however, was extremely well protected. The microarray studies in rodents that have prospected the adaptive response to fasting of the small intestine (13), liver (14, 48), and muscle (21, 49, 50) and

[3] The abbreviations used are: *Pck1*, phosphoenolpyruvate carboxykinase 1; AP-1, transcription factor AP-1 (protein superfamily); CAR, constitutive androstane receptor (nuclear receptor subfamily 1, group I, member 3, Nr1i3); *Cdkn1a*, cyclin-dependent kinase inhibitor 1A (p21); C-MYC, myelocytomatosis oncogene; *Dhcr7*, 7-dehydrocholesterol reductase; *FoxO*, forkhead box O; *G6pc*, glucose-6-phosphatase; *Hmgcr*, 3-hydroxy-3-methyl-glutaryl-CoA reductase; *Hnf4a*, hepatic nuclear factor 4 α (nuclear receptor subfamily 2, group A, member 1; Nr2a1); *Lrh*, liver receptor homolog 1 (nuclear receptor subfamily 5, group A, member 2 Nr5a2); *Pgc-1α*, peroxisome proliferative activated receptor, γ, coactivator 1α; PPARα, peroxisome proliferator-activated receptor α (nuclear receptor subfamily 1, group C, member 1; Nr1c1); *Pxr*, pregnane X receptor (nuclear receptor subfamily 1, group I, member 2; Nr1i2); *Rarβ*, retinoic acid receptor β; *Rorα*, RAR-related orphan receptor α (nuclear receptor subfamily 1, group F, member 1; Nr1f1); *Rorγ*, RAR-related orphan receptor γ; SP1, trans-acting transcription factor 1; AR, androgen receptor; c-Jun, Jun oncogene; EGF, epidermal growth factor; EGR, early growth response; GCR, glucocorticoid receptor, Nr3c1; SREBP, sterol regulatory element binding transcription factor.

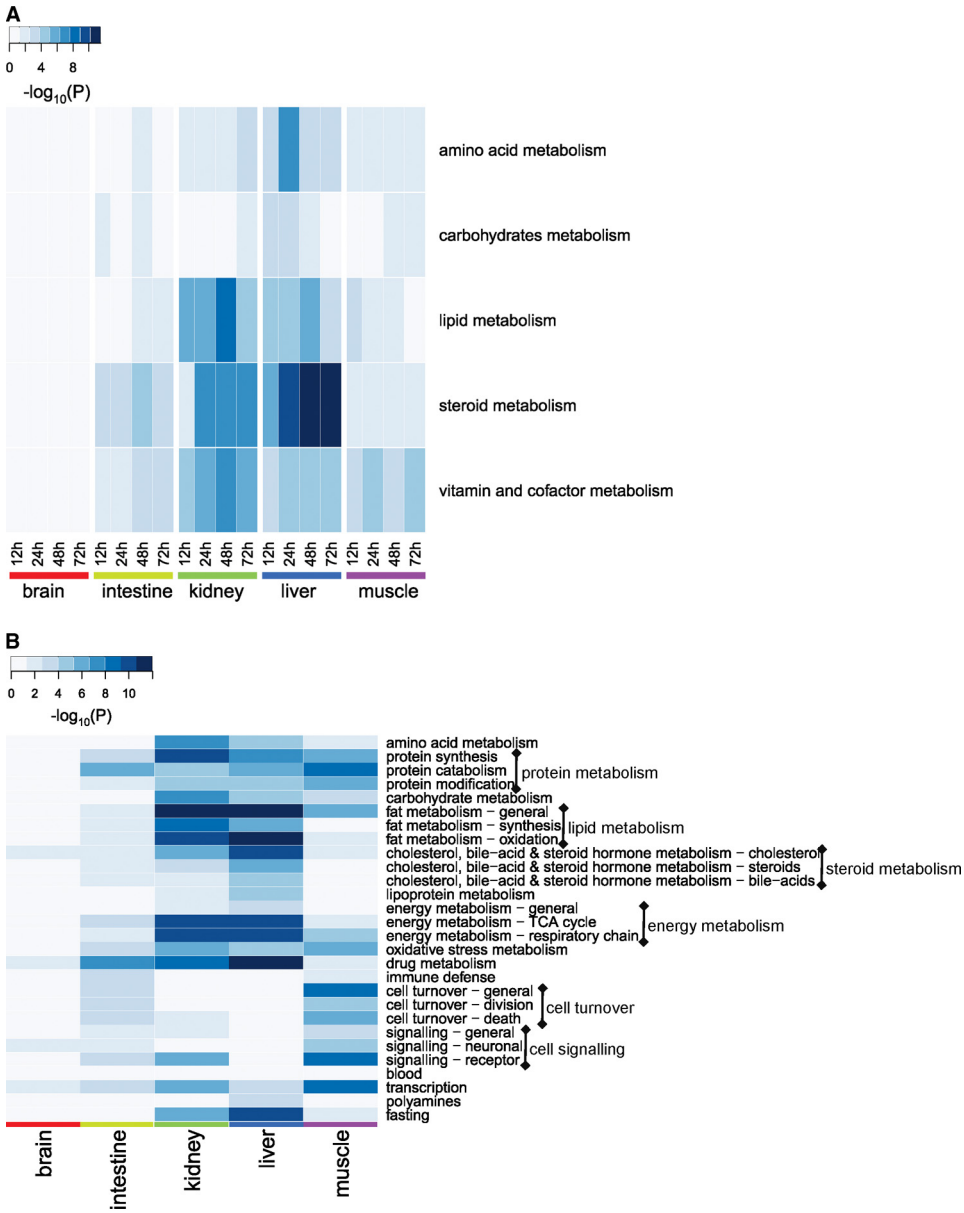

FIGURE 4. **Interorgan similarities and differences in metabolic processes affected by fasting.** *Panel A*, shown is spatiotemporal distribution of significantly regulated processes (as defined in the MetaCoreTM suit) after functional-category enrichment analysis. The heat map visualizes significantly regulated processes (*y* axis) in each of the organs at different time points of fasting (*x* axis). *Panel B*, higher order keywords enriched by fasting as produced by CoPub keyword-enrichment analysis are shown. The heat map shows the level of significance of 28 higher order categories keywords for each of the organs for the whole duration of fasting. Color intensity depicts the significance of the change expressed as the negative logarithm of *p* values obtained in both analyses. *TCA*, tricarboxylic acid cycle.

the current multiorgan study, therefore, reveal a scenario that differs from the "sugars-fats-proteins" succession of energy substrates. For the whole body, this sequence of substrates was proposed to characterize the postabsorptive, coping, and preterminal phases of the adaptation to fasting, respectively (18, 51). Within hours after the last meal, the organs respond with changes in gene expression. In this "early response," adaptive changes in general metabolism prevail that include carbohydrate, fat, and protein metabolism, although the most prominent response occurred in lipid and steroid metabolism. After 24 h of fasting, the temporary early response is replaced by a response focused on a slow-down of cell turnover and immune responses.

In agreement with a requirement for the preservation of glucose for cell types that are exclusively dependent on it (most importantly, brain and erythrocytes (52)), all forms of fatty acid oxidation were impressively up-regulated under control of *Pparα* (liver, kidney, intestines, and muscle) and *Pgc1α* (kidney and muscle). This response was not restricted to muscle and liver (53, 54); it started shortly after the beginning of the fast in all four organs and persisted into the late response. Fatty acid oxidation was accompanied by a strong increase in expression of genes involved in ketone body synthesis in the small intestine, kidney, and liver, a property thus far hardly ascribed to the intestine (55, 56). At the same time, expensive cholesterol synthesis was strictly controlled by down-regulation of the genes encoding key synthetic enzymes (*e.g. Hmgcr* and *Dhcr*) in liver and kidney (supplemental File 3). Up-regulation of the bile-acid synthesis pathway in the kidney does not imply that this organ

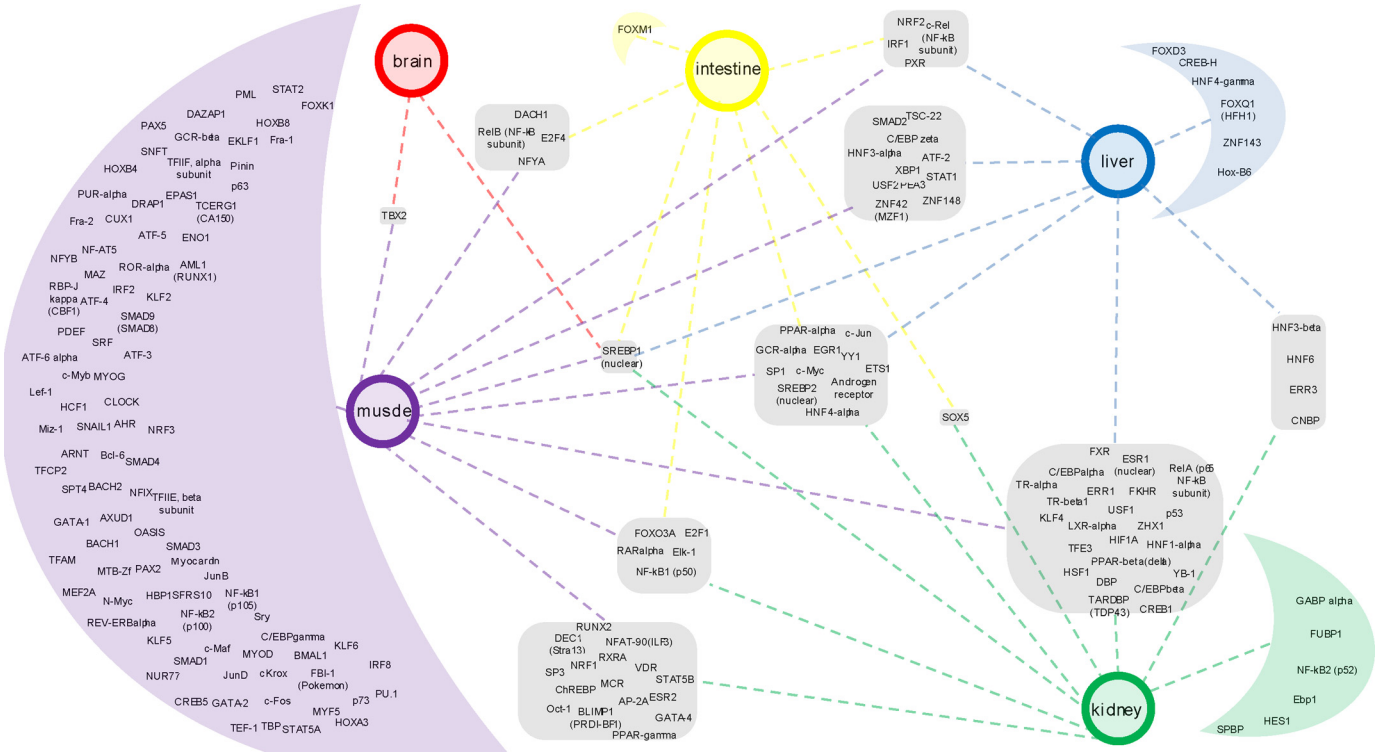

FIGURE 5. **Common and organ-specific transcriptional regulators of the fasting response.** Overconnectivity of transcription factors (the nodes of the primary networks of differentially regulated genes) was calculated for each organ using MetaCore Interactome analysis. The resulting network of common and organ-specific regulators was created and visualized in Cytoscape and enhanced in Adobe Illustrator. The tissues are represented with *colored circles*. Transcription factors, grouped according to the organs for which they are common or specific, are depicted in corresponding *rounded squares/half-moons*, respectively.

produces bile acids but reflects an adaptation in sterol metabolism in response to fasting. Hydroxylation of cholesterol at the 27 position by the mitochondrial sterol 27-hydroxylase (2-fold up-regulated, supplemental File 3), for instance, may serve to regulate the mitochondrial cholesterol content (57). The body limits the loss of cholesterol by a dramatic decrease in fecal cholesterol excretion, whereas biliary output increases to provide the essential luminal nourishment to the enterocytes and keep them viable for when food becomes again available (15). Down-regulation of genes involved in synthesis of ceramides and complex (glyco)sphingolipids in kidney and muscle also became apparent from our Gene Ontology enrichment analysis (data not shown). Although this decline can be explained by the lack of precursors (58), it nonetheless indicates a strict transcriptional regulation of insulin signaling in fasting at the level of membrane organization. Also in brain, despite its limited transcriptomics response to fasting, genes involved in cholesterol biosynthesis were down-regulated. Given the significance of intrinsic cholesterol biosynthesis in brain (59, 60) and the fact that changes in cholesterol homeostasis lead to a wide variety of central nervous system disorders (61), the change in the cholesterol synthesis pathway may point to increased vulnerability of neuronal membranes (62), leading to brain damage that eventually occurs as a consequence of starvation (63).

The text mining analyses drew our attention to *Foxo1* and *Foxo3a* transcription factors, which otherwise could have passed unnoticed, whereas the Interactome analysis revealed four other members of the forkhead gene family as additional regulators of the fasting response. FOXO transcription factors regulate responses to oxidative stress, differentiation, cell-cycle arrest, and cell death (40, 64, 65). They also control gluconeogenesis (via regulation of *Pck1* and *G6pc*) and muscle atrophy (in conjunction with *Fbxo32*) (64–67). In addition, hypothalamic FOXO1 regulates food intake and energy homeostasis (by inhibiting leptin-induced gene transcription (68, 69)). In support of the role of FOXOs as cell fate controllers, cell proliferation and apoptosis were heavily regulated in the fasted small intestine and muscle. Interestingly, *Foxo3a* was not found regulated in the fasted brain, but p21, which is activated by it (70), was. Given the wide variety of their diverse binding partners (71), especially PPARs, that are involved in nutrient sensing and regulation of metabolism, it is tempting to suggest a major role for the FOXO transcription factors in a coordinated interorgan response to fasting.

The network and Interactome analyses highlighted a number of transcription factors as the major regulator of overall adaptation to fasting in mice. The prominence of members of the nuclear receptor family is striking, accounting for almost a quarter of all common transcription factors. These factors are predominantly present in kidney, liver, and muscle. HNF4α coordinated the liver response to fasting. It triggers pleiotropic effects on lipid metabolism, glucose homeostasis, and inflammation and is a central regulator in the network of nuclear receptors that integrates liver intermediate metabolism (72). Kidney response to fasting was, among others, orchestrated by EGF signaling, which regulates cell turnover, cell adhesion, inflammation, and matrix remodeling (73). EGF signaling via EGR is heavily influenced by changes in membrane lipid composition (74), likely to occur in fasting conditions, further highlighting the importance of strict control of cho-

lesterol levels. Further supporting the findings linked to regulation of lipid metabolism, the overconnectivity of SREBP1 was identified in all organs studied. This promiscuous transcriptional activator is essential for lipid homeostasis (as it regulates fatty acid, phospholipid, and to a lesser degree, cholesterol metabolism) but also regulates the non-lipid pathways and was recently suggested to play a crucial role in maintenance of membrane lipid homeostasis (75). AR, a prominent hub in all the metabolically active fasting tissues, plays a role in cellular proliferation, survival, lipid metabolism, and differentiation (76). GCR affects inflammatory responses, cellular proliferation, and differentiation in target tissues (77). Along the same line, one of the most prominent hubs in the small intestine networks, AP-1 transcription factors, regulate transcription of genes involved in cellular proliferation, differentiation, apoptosis, and transformation (78, 79). In muscle, SP1, c-MYC, and AP-1 (both c-JUN and c-FOS) were the main regulators of adaptation to fasting. SP1 regulates the expression of numerous genes implicated in the control of cell growth, differentiation, apoptosis, angiogenesis, and immune response (80) while efficiently transducing insulin signaling to the nucleus (81, 82). AP-1 and c-MYC proto-oncogenes are also essential components of cell proliferative machinery (83). The transcription factors identified by this study indicate an integrated response of lipid metabolism and cell turnover as the hallmark of overall adaptation to fasting.

Finally, using the systems biology approach, we were able to demonstrate at the transcriptome level what has been *a priori* intuitively acknowledged; that is, the extreme protection of the brain from the effects of prolonged fasting. Not many genes were differentially expressed, with most of the changes occurring after prolonged fasting. The switch to ketone body utilization is most likely brought about by the increasing level of β-hydroxybutyrate alone (84) without an accompanying increase in enzymes or transporters.

Acknowledgments—Bioinformatics was part of the BioRange program of the Netherlands Bioinformatics Center, supported by an Investment Grants for Knowledge Infrastructure grant through the Netherlands Genomics Initiative. The microarrays were provided and hybridizations were performed by MicroArray Department, Swammerdam Institute for Life Sciences, Faculty of Science, University of Amsterdam. We are indebted to Dr. N. Dabhoiwala (Department of Urology, Academic Medical Center, University of Amsterdam) and the John Emmett Foundation for Urology for financing a part of the microarray analysis. We thank D. Wehkamp and Dr. L. Gilhuijs-Pederson for input into the initial design of the experiment, Dr. M. Swat for useful suggestions for data visualization, Dr. Y. Nikolsky for support with MetaCore analyses, Dr. S. M. Houten for β-hydroxybutyrate measurement, and Prof. Dr. A. K. Groen and Dr. C. A. Argmann for constructive discussions.

REFERENCES

1. Diamond, J. (2003) *Nature* **423,** 599–602
2. Södersten, P., Bergh, C., and Zandian, M. (2006) *Horm. Behav.* **50,** 572–578
3. Cahill, G. F., Jr. (2006) *Annu. Rev. Nutr.* **26,** 1–22
4. Owen, O. E., Felig, P., Morgan, A. P., Wahren, J., and Cahill, G. F., Jr. (1969) *J. Clin. Invest.* **48,** 574–583
5. Felig, P., Owen, O. E., Wahren, J., and Cahill, G. F., Jr. (1969) *J. Clin. Invest.* **48,** 584–594
6. Felig, P., Marliss, E., Pozefsky, T., and Cahill, G. F., Jr. (1970) *Am. J. Clin. Nutr.* **23,** 986–992
7. Hannaford, M. C., Leiter, L. A., Josse, R. G., Goldstein, M. B., Marliss, E. B., and Halperin, M. L. (1982) *Am. J. Physiol.* **243,** E251–E256
8. Reichard, G. A., Jr., Owen, O. E., Haff, A. C., Paul, P., and Bortz, W. M. (1974) *J. Clin. Invest.* **53,** 508–515
9. Garber, A. J., Menzel, P. H., Boden, G., and Owen, O. E. (1974) *J. Clin. Invest.* **54,** 981–989
10. Sigler, M. H. (1975) *J. Clin. Invest.* **55,** 377–387
11. Owen, O. E., Morgan, A. P., Kemp, H. G., Sullivan, J. M., Herrera, M. G., and Cahill, G. F., Jr. (1967) *J. Clin. Invest.* **46,** 1589–1595
12. Owen, O. E., Smalley, K. J., D'Alessio, D. A., Mozzoli, M. A., and Dawson, E. K. (1998) *Am. J. Clin. Nutr.* **68,** 12–34
13. Sokolović, M., Wehkamp, D., Sokolović, A., Vermeulen, J., Gilhuijs-Pederson, L. A., van Haaften, R. I., Nikolsky, Y., Evelo, C. T., van Kampen, A. H., Hakvoort, T. B., and Lamers, W. H. (2007) *BMC Genomics* **8,** 361
14. Sokolović, M., Sokolović, A., Wehkamp, D., Ver, Loren, van Themaat, E., de Waart, D. R., Gilhuijs-Pederson, L. A., Nikolsky, Y., van Kampen, A. H., Hakvoort, T. B., and Lamers, W. H. (2008) *BMC Genomics* **9,** 528
15. Sokolović, M., Sokolović, A., van Roomen, C. P., Gruber, A., Ottenhoff, R., Scheij, S., Hakvoort, T. B., Lamers, W. H., and Groen, A. K. (2010) *J. Hepatol.* **52,** 737–744
16. He, Y., Hakvoort, T. B., Köhler, S. E., Vermeulen, J. L., de Waart, D. R., de Theije, C., ten Have, G. A., van Eijk, H. M., Kunne, C., Labruyere, W. T., Houten, S. M., Sokolovic, M., Ruijter, J. M., Deutz, N. E., and Lamers, W. H. (2010) *J. Biol. Chem.* **285,** 9516–9524
17. Schreiber, R. A., and Yeh, Y. Y. (1984) *Drug Alcohol Depend.* **13,** 151–160
18. Le Maho, Y., Vu Van Kha, H., Koubi, H., Dewasmes, G., Girard, J., Ferré, P., and Cagnard, M. (1981) *Am. J. Physiol.* **241,** E342–E354
19. Cherel, Y., Attaix, D., Rosolowska-Huszcz, D., Belkhou, R., Robin, J. P., Arnal, M., and Le Maho, Y. (1991) *Clin. Sci.* **81,** 611–619
20. Habold, C., Foltzer-Jourdainne, C., Le Maho, Y., Lignot, J. H., and Oudart, H. (2005) *J. Physiol.* **566,** 575–586
21. Jagoe, R. T., Lecker, S. H., Gomes, M., and Goldberg, A. L. (2002) *FASEB J.* **16,** 1697–1712
22. Habold, C., Foltzer-Jourdainne, C., Le Maho, Y., and Lignot, J. H. (2006) *Pflugers Archiv* **451,** 749–759
23. Dobbin, K., and Simon, R. (2002) *Bioinformatics* **18,** 1438–1445
24. Jonker, M. J., Bruning, O., van Iterson, M., Schaap, M. M., van der Hoeven, T. V., Vrieling, H., Beems, R. B., de Vries, A., van Steeg, H., Breit, T. M., and Luijten, M. (2009) *Carcinogenesis* **30,** 1805–1812
25. Edgar, R., Domrachev, M., and Lash, A. E. (2002) *Nucleic Acids Res.* **30,** 207–210
26. Gentleman, R. C., Carey, V. J., Bates, D. M., Bolstad, B., Dettling, M., Dudoit, S., Ellis, B., Gautier, L., Ge, Y., Gentry, J., Hornik, K., Hothorn, T., Huber, W., Iacus, S., Irizarry, R., Leisch, F., Li, C., Maechler, M., Rossini, A. J., Sawitzki, G., Smith, C., Smyth, G., Tierney, L., Yang, J. Y., and Zhang, J. (2004) *Genome Biol.* **5,** R80
27. Ritchie, M. E., Silver, J., Oshlack, A., Holmes, M., Diyagama, D., Holloway, A., and Smyth, G. K. (2007) *Bioinformatics* **23,** 2700–2707
28. Smyth, G. K. (2004) *Stat. Appl. Genet. Mol. Biol.* **3,** Article 3
29. Ekins, S., Kirillov, E., Rakhmatulin, E. A., and Nikolskaya, T. (2005) *Drug Metab. Dispos.* **33,** 474–481
30. Nikolsky, Y., Nikolskaya, T., and Bugrim, A. (2005) *Drug Discov. Today* **10,** 653–662
31. Nikolsky, Y., Kirillov, E., Zuev, R., Rakhmatulin, E., and Nikolskaya, T. (2009) *Methods Mol. Biol.* **563,** 177–196
32. Piruzian, E., Bruskin, S., Ishkin, A., Abdeev, R., Moshkovskii, S., Melnik, S., Nikolsky, Y., and Nikolskaya, T. (2010) *BMC. Syst. Biol.* **4,** 41
33. Shannon, P., Markiel, A., Ozier, O., Baliga, N. S., Wang, J. T., Ramage, D., Amin, N., Schwikowski, B., and Ideker, T. (2003) *Genome Res.* **13,** 2498–2504
34. Frijters, R., Verhoeven, S., Alkema, W., van Schaik, R., and Polman, J. (2007) *Pharmacogenomics* **8,** 1521–1534
35. Frijters, R., Heupers, B., van Beek, P., Bouwhuis, M., van Schaik, R., de Vlieg, J., Polman, J., and Alkema, W. (2008) *Nucleic Acids Res.* **36,** W406–W410
36. Alako, B. T., Veldhoven, A., van, Baal, S., Jelier, R., Verhoeven, S., Rul-

lmann, T., Polman, J., and Jenster, G. (2005) *BMC. Bioinformatics* **6,** 51
37. Ashburner, M., Ball, C. A., Blake, J. A., Botstein, D., Butler, H., Cherry, J. M., Davis, A. P., Dolinski, K., Dwight, S. S., Eppig, J. T., Harris, M. A., Hill, D. P., Issel-Tarver, L., Kasarskis, A., Lewis, S., Matese, J. C., Richardson, J. E., Ringwald, M., Rubin, G. M., and Sherlock, G. (2000) *Nat. Genet.* **25,** 25–29
38. Hegardt, F. G. (1999) *Biochem. J.* **338,** 569–582
39. Mithieux, G. (2005) *Curr. Opin. Clin. Nutr. Metab. Care* **8,** 445–449
40. Olmos, Y., Valle, I., Borniquel, S., Tierrez, A., Soria, E., Lamas, S., and Monsalve, M. (2009) *J. Biol. Chem.* **284,** 14476–14484
41. Hall, R. K., Yamasaki, T., Kucera, T., Waltner-Law, M., O'Brien, R., and Granner, D. K. (2000) *J. Biol. Chem.* **275,** 30169–30175
42. Salih, D. A., and Brunet, A. (2008) *Curr. Opin. Cell Biol.* **20,** 126–136
43. Hirota, K., Sakamaki, J., Ishida, J., Shimamoto, Y., Nishihara, S., Kodama, N., Ohta, K., Yamamoto, M., Tanimoto, K., and Fukamizu, A. (2008) *J. Biol. Chem.* **283,** 32432–32441
44. Kadowaki, T., and Yamauchi, T. (2005) *Endocr. Rev.* **26,** 439–451
45. Guillod-Maximin, E., Roy, A. F., Vacher, C. M., Aubourg, A., Bailleux, V., Lorsignol, A., Pénicaud, L., Parquet, M., and Taouis, M. (2009) *J. Endocrinol.* **200,** 93–105
46. Gatti, D., Maki, A., Chesler, E. J., Kirova, R., Kosyk, O., Lu, L., Manly, K. F., Williams, R. W., Perkins, A., Langston, M. A., Threadgill, D. W., and Rusyn, I. (2007) *Hepatology* **46,** 548–557
47. Koutnikova, H., Laakso, M., Lu, L., Combe, R., Paananen, J., Kuulasmaa, T., Kuusisto, J., Häring, H. U., Hansen, T., Pedersen, O., Smith, U., Hanefeld, M., Williams, R. W., and Auwerx, J. (2009) *PLoS Genet.* **5,** e1000591
48. Bauer, M., Hamm, A. C., Bonaus, M., Jacob, A., Jaekel, J., Schorle, H., Pankratz, M. J., and Katzenberger, J. D. (2004) *Physiol. Genomics* **17,** 230–244
49. Lecker, S. H., Jagoe, R. T., Gilbert, A., Gomes, M., Baracos, V., Bailey, J., Price, S. R., Mitch, W. E., and Goldberg, A. L. (2004) *FASEB J.* **18,** 39–51
50. Xiao, X. Q., Grove, K. L., and Smith, M. S. (2004) *Endocrinology* **145,** 5344–5354
51. Caloin, M. (2004) *Am. J. Physiol. Endocrinol. Metab* **287,** E790–E798
52. Randle, P. J., Priestman, D. A., Mistry, S. C., and Halsall, A. (1994) *J. Cell. Biochem.* **55,** 1–11
53. Henriksson, J. (1990) *Eur. J. Clin. Nutr.* **44,** 55–64
54. Finn, P. F., and Dice, J. F. (2006) *Nutrition* **22,** 830–844
55. Hegardt, F. G. (1998) *Biochimie* **80,** 803–806
56. VanItallie, T. B., and Nufert, T. H. (2003) *Nutrition Reviews* **61,** 327–341
57. Ning, Y., Bai, Q., Lu, H., Li, X., Pandak, W. M., Zhao, F., Chen, S., Ren, S., and Yin, L. (2009) *Atherosclerosis* **204,** 114–120
58. Langeveld, M., and Aerts, J. M. (2009) *Prog. Lipid Res.* **48,** 196–205
59. Jurevics, H., and Morell, P. (1995) *J. Neurochem.* **64,** 895–901
60. Korade, Z., Kenworthy, A. K., and Mirnics, K. (2009) *J. Neurosci. Res.* **87,** 866–875
61. Maxfield, F. R., and Tabas, I. (2005) *Nature* **438,** 612–621
62. Wallner, B., and Machatschke, I. H. (2009) *Prog. Neuropsychopharmacol. Biol. Psychiatry* **33,** 391–397
63. Auer, R. N. (2004) *Metab. Brain Dis.* **19,** 169–175
64. Arden, K. C. (2008) *Oncogene* **27,** 2345–2350
65. Carter, M. E., and Brunet, A. (2007) *Curr. Biol.* **17,** R113–R114
66. Kandarian, S. C., and Jackman, R. W. (2006) *Muscle Nerve* **33,** 155–165
67. Cao, P. R., Kim, H. J., and Lecker, S. H. (2005) *Int. J. Biochem. Cell Biol.* **37,** 2088–2097
68. Kim, M. S., Pak, Y. K., Jang, P. G., Namkoong, C., Choi, Y. S., Won, J. C., Kim, K. S., Kim, S. W., Kim, H. S., Park, J. Y., Kim, Y. B., and Lee, K. U. (2006) *Nat. Neurosci.* **9,** 901–906
69. Yang, G., Lim, C. Y., Li, C., Xiao, X., Radda, G. K., Li, C., Cao, X., and Han, W. (2009) *J. Biol. Chem.* **284,** 3719–3727
70. Seoane, J., Le, H. V., Shen, L., Anderson, S. A., and Massagué, J. (2004) *Cell* **117,** 211–223
71. van der Vos, K. E., and Coffer, P. J. (2008) *Oncogene* **27,** 2289–2299
72. Desvergne, B., Michalik, L., and Wahli, W. (2006) *Physiol. Rev.* **86,** 465–514
73. D'Alessio, S., and Blasi, F. (2009) *Front Biosci.* **14,** 4575–4587
74. Freeman, M. R., Cinar, B., Kim, J., Mukhopadhyay, N. K., Di Vizio, D., Adam, R. M., and Solomon, K. R. (2007) *Steroids* **72,** 210–217
75. Hagen, R. M., Rodriguez-Cuenca, S., and Vidal-Puig, A. (2010) *FEBS Lett.* **584,** 2689–2698
76. Lamont, K. R., and Tindall, D. J. (2010) *Adv. Cancer Res.* **107,** 137–162
77. Rogatsky, I., and Ivashkiv, L. B. (2006) *Tissue Antigens* **68,** 1–12
78. Hess, J., Angel, P., and Schorpp-Kistner, M. (2004) *J. Cell Sci.* **117,** 5965–5973
79. Vesely, P. W., Staber, P. B., Hoefler, G., and Kenner, L. (2009) *Mutat. Res.* **682,** 7–12
80. Tan, N. Y., and Khachigian, L. M. (2009) *Mol. Cell. Biol.* **29,** 2483–2488
81. Solomon, S. S., Majumdar, G., Martinez-Hernandez, A., and Raghow, R. (2008) *Life Sci.* **83,** 305–312
82. Mounier, C., and Posner, B. I. (2006) *Can. J. Physiol Pharmacol.* **84,** 713–724
83. Zajac-Kaye, M. (2001) *Lung Cancer* **34,** S43–S46
84. Veech, R. L. (2004) *Prostaglandins Leukot. Essent. Fatty Acids* **70,** 309–319